

1

2

3

4

5 **Catecholaminergic modulation of large-scale network dynamics is tied to the**  
6 **reconfiguration of corticostriatal connectivity**

7 **Justine A. Hill<sup>1</sup>, Cole Korponay<sup>2,3</sup>, Betty Jo Salmeron<sup>1</sup>, Thomas J. Ross<sup>1</sup>, Amy C. Janes<sup>1</sup>**

8 **<sup>1</sup> National Institute on Drug Abuse Intramural Research Program**

9 **Biomedical Research Center 251 Bayview Blvd. 7A Baltimore, MD 21224**

10 **<sup>2</sup> McLean Hospital, Belmont, MA**

11 **<sup>3</sup> Harvard Medical School, Boston, MA**

12 **Phone: 667-312-5146**

13 **Email: [Justine.hill@nih.gov](mailto:Justine.hill@nih.gov)**

14 **Running Title: Catecholamine impact on network temporal dynamics**

15 ***ABSTRACT***

16 Large-scale brain network function is critical for healthy cognition, yet links between such  
17 network function, neurochemistry, and smaller-scale neurocircuitry are unclear. Here, we  
18 evaluated 59 healthy individuals using resting-state fMRI to determine how network-level  
19 temporal dynamics were impacted by two well-characterized pharmacotherapies targeting  
20 catecholamines: methylphenidate (20mg) and haloperidol (2mg). Network dynamic changes  
21 were tested for links with drug-induced alterations in complex corticostriatal connections as this  
22 circuit is a primary site of action for both drugs. A randomized, double-blind, placebo-controlled  
23 design was used. Methylphenidate enhanced time spent in the default mode network (DMN  $p < 0$   
24  $.001$ ) and dorsal attention network (DAN  $p < 0.001$ ) and reduced time in the frontoparietal  
25 network ( $p < 0.01$ ). Haloperidol increased time in a sensory motor-DMN state ( $p < 0.01$ ). The  
26 magnitude of change in network dynamics induced by methylphenidate vs. placebo was  
27 correlated with the magnitude of methylphenidate-induced rearrangement of  
28 complex corticostriatal connectivity ( $R = 0.32$ ,  $p = 0.014$ ). Haloperidol did not alter  
29 complex corticostriatal connectivity. Methylphenidate increased time in networks involved in  
30 internal (DMN) and external attention (DAN), aligning with methylphenidate's established role  
31 in attention. Methylphenidate also significantly changed complex corticostriatal connectivity by  
32 altering the relative strength between multiple corticostriatal connections, indicating that  
33 methylphenidate may shift which corticostriatal connections are prioritized relative to others.  
34 Findings further show that these local circuit changes are linked with large scale network  
35 function. Collectively, these findings provide a deeper understanding of large-scale network  
36 function, set a stage for mechanistic understanding of network engagement, and provide needed  
37 information to potentially guide medication use based on network-level effects.

## 38 **Introduction**

39 Resting-state brain networks have provided critical insight into the macro-scale  
40 functional organization of the brain, which is implicated in healthy cognition and  
41 psychopathology(1–3). A key next step is to understand how the function of these distributed  
42 brain networks correspond with changes in neurochemistry and more focal functional circuits.  
43 While catecholamines, such as dopamine, have been implicated in large-scale network  
44 function(3–6), more work using emerging methods is needed to gain a deeper understanding of  
45 how catecholaminergic agents impact large-scale network function. Collectively, this line of  
46 research promises to enhance the field’s basic neurobiological understanding of brain network  
47 function and will shed light on how well-characterized therapeutics impact the brain on a new  
48 scale.

49 A novel approach to assess how catecholamines modulate large-scale network function is  
50 network temporal dynamics, which is measured using resting-state functional magnetic  
51 resonance imaging (fMRI) data. In contrast to static resting state fMRI analyses which calculates  
52 the functional connectivity between brain regions across time, thus leading to one value for the  
53 entire resting-state scan, temporal dynamics capture how brain network engagement changes  
54 across time. The *resting-state* temporal dynamics of large-scale brain networks have been shown  
55 to be central to adaptive functioning, as aberrance in resting-state network temporal dynamics is  
56 implicated in numerous forms of psychopathology including ADHD(7,8), nicotine  
57 dependence(9–11), cocaine use disorder(12) and schizophrenia(13,14). Dopaminergic  
58 transmission has been directly implicated in one *task-based* analysis of network temporal  
59 dynamics, which demonstrated that dopamine modulates the dynamics of brain state transitions  
60 relevant to working memory(4). However, the evidence linking catecholaminergic transmission

61 to resting-state network dynamics is less clear. One study in children with ADHD indicated that  
62 the dopamine and norepinephrine agonist methylphenidate normalized disrupted network  
63 temporal dynamics at rest(8). The remaining evidence linking catecholamines and resting-state  
64 network temporal dynamics is indirect but widespread, where aberrant catecholaminergic  
65 transmission – particularly dopaminergic transmission – is thought to be a principal disruption in  
66 many psychopathologies which reliably exhibit altered network dynamics(7–14) . Taken  
67 together, the direct influence of catecholaminergic transmission on the intrinsic temporal  
68 function of the brain’s large-scale networks (e.g., temporal function at rest) remains largely  
69 unknown, creating a gap in our understanding of how neuromodulators govern this central  
70 component of macro-scale brain function.

71 Our previous work in healthy young adults from the Human Connectome Project used  
72 coactivation pattern analysis (CAP) to define eight transient brain states which include well  
73 defined core neurocognitive networks (e.g., the default mode network (DMN), frontoparietal  
74 network (FPN), and dorsal attention network (DAN))(15). Here, we apply these state definitions  
75 to investigate how acute administration of catecholaminergic agents affect the temporal  
76 properties of large-scale brain networks during resting-state fMRI scans in healthy adults.  
77 Specifically, in one scan condition we administered methylphenidate (MPH), a dopamine and  
78 norepinephrine transporter (DAT/NET) reuptake inhibitor which acts globally to increase  
79 extracellular dopamine and norepinephrine and has been shown to enhance cognition due to  
80 MPH’s impact on striatal function(16–19). In a second scan condition, we administered  
81 haloperidol (HAL), a selective antagonist of D2/D3 receptors located primarily in the striatum.  
82 In a third scan condition, we administered placebo. These drugs were administered randomly

83 across participants and allowed us to probe the impact of catecholaminergic agonism (MPH) and  
84 D2 antagonism (HAL) on temporal dynamics of large-scale brain networks.

85

86 We then move further to investigate ties between catecholaminergic modulation of  
87 macro-scale brain network temporal dynamics and more focal circuitry. On the circuit-level,  
88 catecholamines, most notably dopamine, are known to act directly on the striatum and alter  
89 connectivity between the striatum and the cortex(20). Though most work in fMRI simplifies  
90 corticostriatal communication as connectivity between one striatal node and one cortical node,  
91 corticostriatal circuitry is much more complex. Striatal nodes project to various cortical regions,  
92 while in turn, several cortical regions provide collective and summative input onto striatal  
93 nodes(21,22). Preclinical data supports the notion that striatal function is shaped by the  
94 convergence of multiple cortical inputs rather than input from any one cortical node  
95 alone(21,23). Moreover, the role of striatal dopamine (modulated by both MPH and HAL) may  
96 be to alter how *multiple inputs* are *integrated* at striatal cells(20). As such, here we conduct  
97 connectivity profile analysis(24) to characterize how MPH and HAL alter multifaceted  
98 corticostriatal configuration profiles. We ultimately aim to determine whether the magnitude of  
99 catecholamine-driven change in corticostriatal configuration profiles is tied to the magnitude of  
100 catecholaminergic modulation of network temporal dynamics. Altogether, our design allows us  
101 to establish how dopamine/norepinephrine agonism and D2 antagonism directly impact the  
102 inherent temporal function of macro-level brain networks and how this is tied to modulation of  
103 specific corticostriatal circuitry.

## 104 **Methods and Materials**

### 105 **Participants**

106 Participants included 59 healthy right-handed individuals between the ages 18-55 (Table  
107 1). Participants were excluded for contraindications with fMRI scanning. Individuals with mental  
108 and physical health diagnoses and/or medications that interfere with the bold signal or alter  
109 metabolism of catecholaminergic agents were also excluded (See Supplement for details).  
110 Participants were recruited from Baltimore, MD, and surrounding areas. The current study was  
111 reviewed and approved by the institutional review board of the National Institutes of Health. All  
112 participants provided written informed consent.

### 113 **Study Design**

114 All participants underwent resting-state fMRI scanning sessions with 3 drug conditions  
115 administered on separate days, in a double-blind placebo-controlled manner: placebo/placebo,  
116 HAL/placebo, placebo/MPH. Doses were 2 mg oral HAL and 20 mg oral MPH. Each scanning  
117 visit was identical and took place at drug peak: 4-hours post HAL/placebo and 1-hour post  
118 MPH/placebo; timed in accordance with absorption rates to ensure high and stable plasma levels  
119 of medication during the scan. Prior to any medication administration, participants completed a  
120 nursing assessment, and following the scan session, participants met again with nursing staff to  
121 assess side effects.

### 122 **Neuroimaging Data**

123 At each scan, data were collected using a Siemens Trio 3T scanner with a 12 channel RF  
124 coil. For high-resolution anatomical scan, multi-planar rapidly acquired gradient echo-structural  
125 images were obtained with the following parameters (TR=1.9s, TE= 3.51ms, slices=208,  
126 matrix=192x256, flip angle 9°, resolution 1.0x1.0x1.0 mm). For the 8-minute resting state scan,  
127 gradient-echo, echo planar images were collected using oblique axial scans 30° from AC-PC

128 with AP phase encoding and the following parameters (TR=2s, TE=27ms, flip=78°, vox  
129 resolution=3.4375x3.4375x4 mm). Total frames were 240 and the first 5 were discarded.

130 Images were processed using FMRIB software library (FSL 6.0.0). Images underwent  
131 brain extraction, registration, spatial smoothing (6mm), high pass temporal filtering (100s), and  
132 motion correction via MCFLIRT. Data were further cleaned to reduce motion artifacts using  
133 Independent Component Analysis via FIX(25,26) through MELODIC. Data were then  
134 standardized to MNI152 brain image using FLIRT.

### 135 **Pharmacological Impact on Network Temporal Dynamics**

136 Previously, Janes et. al(15) performed Co-Activation Pattern Analysis (CAPs) on resting  
137 state data from 462 individuals in the Human Connectome Project(27) using 129 ROIs (cortical  
138 and striatal ROIs based on functional parcellation(28,29); amygdala ROIs based on anatomical  
139 parcellation(30)) and determined eight co-activation patterns (brain states) using k-means  
140 clustering. These eight brain states align with previously established resting state networks such  
141 as: the DMN, FPN, DAN, SN, and sensorimotor network (SMO) (Supplementary Figure 1). To  
142 investigate how these eight brain states behave dynamically at rest under different  
143 catecholaminergic drugs, we extracted ROI time courses from the 129 ROIs and conducted  
144 CAPs using the Capcalc package (<https://github.com/bbfrederick/capcalc>). The eight states were  
145 used to compute state-specific dynamic measures including: 1) *total time* spent in each state, 2)  
146 number of *transitions* (i.e. entries) into each state, 3) average *persistence* within the state once a  
147 transition into the state had occurred.

148 To determine an effect of drug on temporal dynamics of brain state activity at rest, we ran  
149 a repeated measures ANOVA that tested the drug × brain state interaction on total time.

150 Following a significant drug  $\times$  brain state interaction, we ran eight subsequent repeated measures  
151 ANOVAs, testing effect of drug on total time in each state. In states where there was a  
152 significant drug effect on total time spent in brain state after correcting for multiple comparisons  
153 (Bonferroni corrected:  $.05/8=.00625$ ), two post-hoc paired t-tests compared MPH and HAL to  
154 placebo (Bonferroni corrected:  $.05/2=.025$ ). All ANOVAs and post-hoc t-tests were conducted in  
155 R using the following packages: lme4 (1.1-32), lmerTest (3.1-3), effectsize (0.8.3), and multcomp  
156 (1.4-23). All analyses controlled for age and sex.

157 In brain states which exhibit significant change in total time in state under drug, we  
158 investigated whether changes to total time in state were driven by changes in 1) number of  
159 transitions to the state or 2) persistence within state. We ran separate post-hoc paired t-tests  
160 comparing 1) transitions and 2) persistence between drug of interest to placebo. Post-hoc  
161 analyses were Bonferroni corrected to account for all states tested. See supplementary methods  
162 for detailed description of transition analysis.

### 163 **Ties between Network Temporal Dynamics and Static Network Function**

164 Previous work has theorized that spending more time in the DMN and DAN at opposing  
165 times drives enhanced static DMN-DAN anti-correlation(31) – a known marker of healthy  
166 cognition(32,33). Separate literature consistently shows that MPH enhances static DMN-DAN  
167 anti-correlation(34,35). We aimed to confirm that MPH enhances static DMN-DAN anti-  
168 correlation in our sample and tested the conjecture that static DMN-DAN anti-correlation is  
169 driven by DMN and DAN temporal dynamics. To do so, we obtained DMN-DAN anti-  
170 correlation values by regressing the whole brain 4D data on the spatial patterns of DAN and  
171 DMN states using MATLAB 2022b. Correlation values between each network's time course  
172 were computed and Z-transformed using Fisher's R-to-Z. We then tested effect of drug on



173 DMN-DAN anti-correlation with a repeated measures ANOVA and post-hoc t-tests (Bonferroni  
174 corrected). Next, we tested the relationship between static DMN-DAN anti-correlation and  
175 combined time spent in DMN and DAN, hypothesizing that increased time in DMN and DAN  
176 would be associated with greater magnitude of DMN-DAN anti-correlation (based on previous  
177 proposal(31)). We fit a linear mixed model in R to estimate DMN-DAN anti-correlation score  
178 from time in DMN and DAN state combined (summed), when controlling for age, sex, drug, and  
179 drug  $\times$  time in state interaction.

### 180 **Pharmacological Impact on Corticostriatal Configuration**

181 To detect complex changes in corticostriatal connectivity, we conducted connectivity  
182 profile analysis(24). Striatal function is shaped by the convergence of multiple cortical inputs  
183 more so than by any one cortical node alone(21,23). Here, connectivity profile analysis allowed  
184 us to model the multifaceted input received by striatal nodes from diverse areas of cortex, and  
185 study drug-related changes in the properties of these “corticostriatal configuration profiles”  
186 (CSCPs)(24).

187 To derive CSCPs, time courses were first extracted from each voxel of a striatal  
188 mask(24) and from 53 cortical ROIs (used in CAPs states(15)). Correlation values between time  
189 courses at each striatal voxel and each cortical ROI were calculated, then r values were Z-  
190 transformed using Fisher’s R-to-Z. Next, CSCP metrics were calculated in MATLAB (2022b)  
191 (For details, see Korponay et al (2022), and Supplement). Briefly, CSCP metrics include 1)  
192 *aggregate divergence* (AD): absolute sum of the change in connectivity for each ROI at each  
193 striatal voxel (drug – placebo), acting as a measure of absolute change in magnitude of  
194 connectivity under drug; 2) *rank order rearrangement* (ROR): the absolute sum of change in  
195 order of strength of connectivity for each ROI at each striatal voxel (drug – placebo), acting as a

196 measure of absolute change in relative connectivity under drug; 3) *entropy shift* (ES): change in  
197 distribution of the strength of corticostriatal connectivity values under drug compared to placebo.  
198 Here, CSCPs were conducted entirely within-subject. Because CSCP metrics inherently compare  
199 drug to placebo, we also conducted within-session placebo CSCP metrics for statistical analysis  
200 ( $PBO_{\text{firsthalf}} - PBO_{\text{secondhalf}}$ ). This score compared the first and second half of placebo data. In total,  
201 scores were derived across three conditions: MPH-PBO, HAL-PBO,  $PBO_{\text{firsthalf}} - PBO_{\text{secondhalf}}$ .

202 To determine statistical significance, we calculated subject-wise average scores of each  
203 CSCP metric for each condition. We then ran three repeated measures ANOVAs – one for each  
204 metric (AD, ROR, ES) – comparing the drug conditions (Bonferroni corrected). If significant,  
205 post-hoc t-tests compared MPH-PBO, HAL-PBO and  $PBO_{\text{firsthalf}} - PBO_{\text{secondhalf}}$  (Bonferroni  
206 corrected). Where post-hoc t-test revealed a significant drug effect, we then aimed to identify  
207 specific areas of the striatum which were significantly altered by drug. We computed subject-  
208 level striatal maps of significant CSCP metrics. We then performed a voxel-wise paired t-test  
209 between significant drug-placebo and within-session placebo condition using SPM12.

## 210 **Ties between Modulation of Network Temporal Dynamics and Corticostriatal** 211 **Reconfiguration**

212 We tested whether, under the same drug, significant change in network temporal  
213 dynamics was related to significant alterations in CSCP metrics. To do so, first we calculated one  
214 subject-wise score of absolute change in time spent in states under drug. Absolute change in time  
215 spent in states was derived by summing the absolute value of change in time in each of the eight  
216 states ( $\text{time}_{\text{stateN}} \text{ under drug} - \text{time}_{\text{stateN}} \text{ under placebo}$ ). We then tested the relationship between  
217 subject-wise score of significant CSCP metric and absolute change in time spent in states. Where  
218 there was a significant relationship, we aimed to confirm that this relationship, involving change

219 in time spent in *all* states, was specifically driven by change in time spent in states whose  
220 temporal dynamics were determined to be significantly modulated by drug. The goal of this  
221 confirmation was to parse out which networks are involved in the relationship between temporal  
222 dynamic network properties and functional corticostriatal circuitry. This was assessed by  
223 comparing correlations(36) where x remained CSCP score while y varied as absolute change in:  
224 total time spent in all eight states, total time spent in states significantly altered by drug, and total  
225 time spent in states not significantly altered by drug. See exact equations in supplementary  
226 methods.

227 We conducted further exploratory post-hoc analysis to localize which striatal nodes and  
228 individual networks are involved in significant relationships. In contrast to a CSCP score defined  
229 as the mean CSCP score at *all* striatal voxels per subject, node-specific CSCP scores were  
230 derived from the mean of voxels in each significant striatal node identified in the voxel-wise t-  
231 test. Correlations were calculated between node-specific CSCP scores and change in time spent  
232 in each state significantly modulated by drug.

233

## 234 **Results**

### 235 **Network Temporal Dynamics**

236 We first tested for effect of drug on total time spent in brain states. There was a  
237 significant effect of brain state ( $F(16,928)=19.53, p<0.001$ ) and a drug  $\times$  brain state interaction  
238 ( $F(16,928)=5.78, p<0.001$ ) on total time spent in brain states. A significant effect of drug was  
239 noted for the DMN ( $F(2,116)=15.29, p_{\text{corr}}<0.001, \eta^2=0.21$ ), DAN ( $F(2,116)=12.42, p_{\text{corr}}<0.001$ ,

240  $\eta^2=0.18$ ), FPN ( $F(2,116)=5.95$ ,  $p_{\text{corr}}<0.05$ ,  $\eta^2=0.09$ ) and sensorimotor-occipital DMN (SM-  
241 DMN) state ( $F(2,116)=9.97$ ,  $p_{\text{corr}}<0.001$ ,  $\eta^2=0.15$ ).

242 Post-hoc analysis revealed that relative to placebo, MPH increased time spent in the  
243 DMN ( $p_{\text{corr}}<0.001$ ,  $d=0.74$ ) and DAN states ( $p_{\text{corr}}<0.001$ ,  $d=0.665$ ). Increased time was explained  
244 by MPH increasing the number of transitions into the DMN ( $p_{\text{corr}}<0.001$ ,  $d=0.72$ ) and DAN  
245 states ( $p_{\text{corr}}<0.001$ ,  $d=0.78$ ). In contrast, MPH had no impact on persistence in either state  
246 ( $p_{\text{corr}}>0.05$ ). Given that the DMN and DAN play substantial roles in internal(37–40) and external  
247 attention(37,41), respectively, this finding builds on previous literature of MPH's known role in  
248 attentional enhancement and provides novel insight whereby MPH inherently increases  
249 transitions into attention-related networks. MPH also reduced the time spent in the FPN state  
250 relative to placebo ( $p_{\text{corr}}<0.01$ ,  $d=-0.445$ ) and reduced transitions into this state at a significance  
251 level that did not withstand Bonferroni correction ( $p_{\text{corr}}=0.17$ ) without influencing persistence  
252 ( $p_{\text{corr}}>0.05$ ) (Figure 1A-C).

253 Relative to placebo, HAL increased the time spent in the SM-DMN, which represents the  
254 co-activation of sensory motor regions and the DMN ( $p_{\text{corr}}<0.01$ ,  $d=0.49$ ). HAL increased the  
255 number of transitions into this state ( $p_{\text{corr}}=0.013$ ,  $d=0.48$ ) and increased the persistence within the  
256 SM-DMN at a level that did not withstand Bonferroni correction ( $p_{\text{corr}}=0.054$ ) (Figure 1A-C).  
257 The effect of HAL on sensory motor-related state dynamics fits with previous findings  
258 demonstrating that HAL impacts sensory motor systems(42) and demonstrates that MPH and  
259 HAL impact the inherent temporal function of different large-scale networks.

260 **DAN / DMN Anti-correlation**

261           There was a significant effect of drug on the DMN-DAN anti-correlation ( $F(2,116)=11.6$ ,  
262  $p<0.001$ ,  $\eta^2=0.17$ ). Post-hoc comparisons confirmed that MPH had a significantly greater  
263 magnitude of static DMN-DAN anti-correlation versus placebo (Figure 2A,  $p_{\text{corr}}=0.0014$ ,  
264  $d=0.57$ ) which aligns with previous literature(34,35), whereas HAL did not significantly differ  
265 from placebo ( $p_{\text{corr}}>0.05$ ). We then tested the hypothesis that greater magnitude of static DMN-  
266 DAN anti-correlation could be driven by increased time spent in both the DMN and DAN. Time  
267 in DMN and DAN combined negatively estimated DMN-DAN correlation independently of drug  
268 conditions (Figure 2B,  $p<0.001$ , conditional  $R^2=0.72$ , marginal  $R^2=0.59$ ). This lends significant  
269 evidence towards the conjecture(31) that enhanced anti-correlation of the DMN and DAN is  
270 driven by spending more time both states, at opposing times.

### 271 **Corticostriatal Configurations**

272           We measured catecholaminergic manipulation of corticostriatal circuitry by measuring  
273 effect of drug on CSCP metrics: AD, ROR, and ES. There was a significant effect of drug on  
274 ROR, the measure of absolute change in *relative* corticostriatal connectivity, following repeated  
275 measures ANOVA ( $F(2,116)=15.36$ ,  $p_{\text{corr}}<0.001$ ,  $\eta^2=0.21$ ). There was no effect of drug on AD or  
276 ES ( $p_{\text{corr}}>0.05$ ), which measure the absolute magnitude of change in corticostriatal connectivity  
277 values and change in distribution of the strength of corticostriatal connectivity values,  
278 respectively. Post-hoc comparisons revealed that the MPH-PBO condition exhibited significantly  
279 higher ROR compared to within-session placebo ( $p_{\text{corr}}<0.001$ ,  $d=0.86$ ) and HAL-PBO  
280 ( $p_{\text{corr}}<0.001$ ,  $d=0.73$ ; Figure 3A). There was no difference between HAL-PBO and within-  
281 session placebo ( $p_{\text{corr}}>0.05$ ). This result shows that corticostriatal connectivities which were  
282 relatively weaker under placebo became relatively stronger under methylphenidate and vice  
283 versa, at a statistically significant level when measuring total amount of change in relative

284 strength. Thus, we provide evidence that elevated extracellular dopamine and norepinephrine  
285 alter which specific corticostriatal connections are the strongest or weakest, where this  
286 “*reshuffling*” of the relative connectivity strength of cortical regions with the striatum potentially  
287 reflects a shift in the priority of corticostriatal communications.

288 To localize striatal nodes where MPH significantly induced higher magnitude of ROR  
289 compared to placebo, we conducted a voxel-wise paired t-test of striatal ROR value maps  
290 comparing MPH-PBO to within-session placebo. This revealed five clusters where MPH  
291 significantly induced higher magnitude of ROR compared to placebo: right dorsal caudate; left  
292 dorsal caudate; right nucleus accumbens and ventral caudate; left nucleus accumbens; left ventral  
293 caudate (Supplementary Table 1). See supplementary results for details on how cortical regions  
294 changed in rank order at significant striatal clusters.

### 295 **Network Temporal Dynamics × Corticostriatal Configurations**

296 To determine links between smaller-scale circuitry and the time-varying engagement of  
297 large-scale networks, we tested associations between significant corticostriatal reconfiguration  
298 and change in network temporal dynamics under the same drug. MPH both significantly  
299 increased the absolute change in relative corticostriatal connectivity (ROR) and altered network  
300 temporal dynamics (Figure 1 and 3). We thus tested the association between magnitude of ROR  
301 and change in time spent in network-aligned brain states under MPH. There was a significant  
302 positive relationship between magnitude of ROR (averaged across the entire striatum) and  
303 absolute change in time spent in all brain states under MPH ( $R=0.29$ ,  $p=0.025$ ).

304 We examined whether this relationship was driven by change in time spent in the FPN,  
305 DMN and DAN states, as we determined that MPH significantly altered the time spent in these

306 three states (Figure 1A). There was a significant relationship between magnitude of ROR and  
307 absolute change in time spent in FPN, DMN and DAN states under MPH ( $R=0.32$ ,  $p=0.014$ )  
308 while there was no significant relationship between magnitude of ROR and absolute change in  
309 time spent in all states excluding FPN, DMN and DAN ( $R=0.12$ ,  $p>.05$ ) (Figure 4). The  
310 relationship between magnitude of ROR and absolute change in time spent in all states was  
311 significantly stronger than the relationship involving change in time spent in states *excluding*  
312 FPN, DMN, DAN states ( $z=1.87$ ,  $p=0.031$ ) and not significantly different from the relationship  
313 involving only absolute change in time spent in FPN, DMN and DAN states ( $z=0.37$ ,  $p>0.05$ )  
314 (Figure 4). We thus concluded that MPH-induced change in time spent in FPN, DMN and DAN  
315 combined is principally responsible for the association between MPH-induced change in time  
316 spent in all states and magnitude of corticostriatal ROR.

317 In an exploratory analysis, we aimed to localize specific striatal nodes where magnitude  
318 of ROR may be associated with change in time spent in the FPN, DMN or DAN. We averaged  
319 ROR values for each subject at each of the five striatal nodes previously identified  
320 (Supplementary Table 1). We then tested associations between node-wise ROR and change in  
321 time spent in FPN, DMN and DAN independently – ultimately yielding 15 correlation tests (5  
322 nodes  $\times$  3 brain states). Change in time spent in the DMN alone was significantly positively  
323 related to ROR at the left dorsal striatum (Figure 5B,  $R=0.4$ ,  $p_{\text{uncorr}}=0.0015$ ;  $p_{\text{corr}}=0.0225$ ). The  
324 positive relationship with the right dorsal striatum (Figure 5D,  $R=0.35$ ,  $p_{\text{uncorr}}=0.006$ ,  $p_{\text{corr}}>0.05$ )  
325 did not survive multiple comparisons correction. However, these relationships did not  
326 significantly differ from each other ( $z=-0.87$ ,  $p>0.05$ ). No other relationships were significant  
327 following multiple comparisons correction. These exploratory findings demonstrate that the  
328 magnitude at which MPH reshuffles the relative connectivity strength between different cortical

329 regions and the dorsal caudate is associated with the amount that MPH enhances time spent in  
330 the DMN at rest.

331

## 332 **Discussion**

333 Methylphenidate increased the amount of time spent in the DMN and DAN states by  
334 increasing the frequency of transitions into both states. This finding is compelling given MPH's  
335 known role in attention and the fact that both states play a role in different types of attention.  
336 While the DMN plays a critical role in processes requiring internally focused attention such as  
337 episodic memory(37–40), the DAN is involved in the regulation of external attention, which is  
338 required to meet external task demands(37,41). Thus, even at rest, MPH facilitates dynamic  
339 transitions into attentional states, suggesting that MPH primes the brain to engage in both  
340 internal and external attentional demands. MPH also suppressed the amount of time spent in the  
341 FPN. Previous work has shown that the FPN facilitates goal-directed behavior via flexible  
342 switching between the DMN and the DAN to accomplish an internally or externally oriented  
343 task, respectively(37). Consistent with theories which posit MPH enhances cognitive  
344 efficiency(43), the suppression of time spent in the FPN coupled with enhanced entries into  
345 DMN and DAN may indicate that under MPH, less FPN-related effort is needed to facilitate  
346 goal-directed attention.

347 In a follow-up analysis, we confirmed that in addition to enhancing time spent in DMN  
348 and DAN, MPH strengthens static DMN-DAN anti-correlation. Stronger anti-correlation  
349 between the DMN and the DAN at rest is a known marker of healthy cognition(44), and it has  
350 been hypothesized that increased anti-correlation of these networks is driven by increased time



351 spent in both brain networks, at opposing times(31). Here, we prove this conjecture that a  
352 stronger DMN-DAN anti-correlation is related to increased time in both DMN and DAN states.  
353 Our findings thus show that MPH drives changes in network temporal dynamics which explain  
354 known markers of cognitive enhancement identified by static functional connectivity measures.

355         Pharmacological challenge by HAL, in contrast, increased the amount of time in the SM-  
356 DMN brain state. Though it may appear counterintuitive that both MPH and HAL enhanced time  
357 in DMN-related states, the DMN and SM-DMN states are neurobiologically distinct  
358 representations of co-activated patterns(15). The enhancement of a SM-related network fits with  
359 known effects of antipsychotics on sensorimotor systems(42). Moreover, HAL is used as a first-  
360 line medication to treat schizophrenia, a disorder which exhibits altered temporal function of SM  
361 and DMN(14,45). The current finding in healthy controls that acute HAL enhances temporal  
362 function of two networks temporally disrupted in those with schizophrenia underscores the  
363 necessity of considering pharmacological impact of medication when analyzing temporal  
364 network function in clinical populations. This consideration may clarify mixed findings in the  
365 field(45).

366         Given that MPH and HAL have heightened locus of action at the striatum and act to  
367 modulate large-scale brain networks, we assessed how MPH and HAL impact corticostriatal  
368 function and whether this relates to drug-induced changes in network temporal dynamics. We  
369 obtained CSCPs, which aim to capture complex functional corticostriatal interactions by  
370 quantifying collective and relative connectivity between multiple cortical regions and striatal  
371 nodes, as AD, ROR, and ES. Challenge by HAL had no effect on CSCP measures. Challenge by  
372 MPH, in contrast, altered ROR but did not alter AD or ES. Previous work also has shown that  
373 each configuration property (AD, ROR, ES) is modulated independently and likely represents

374 distinct neurobiological properties which may differentially shape striatal node function(24). We  
375 build on this to show that different pharmacological agents have distinct action on configuration  
376 profiles.

377 In altering ROR alone, MPH specifically acts to *reshuffle* the order of which  
378 corticostriatal connections are relatively greater or weaker at distinct striatal nodes. In doing so,  
379 MPH appears to rearrange the influence that different corticostriatal communications have(46) to  
380 ultimately contribute to altered brain function. It may be, at least in part, that MPH acting at the  
381 striatum significantly alters how cortical input is integrated in striatal cells(20) - though given  
382 MPH's global action and effects on catecholamines broadly, future work is needed to disentangle  
383 this assertion. MPH-induced ROR occurs significantly at bilateral counterparts in the dorsal  
384 caudate and at the right and left nucleus accumbens and ventral caudate. Anatomically, these  
385 striatal nodes are engaged in bi-directional corticostriatal loops(47), and functionally, the dorsal  
386 caudate is tied to FPN while the ventral nodes identified here are linked to the DMN and limbic  
387 network(28).

388 Importantly, we provide novel evidence that MPH-induced corticostriatal ROR is tied to  
389 MPH-induced change in network temporal dynamics. The magnitude of ROR at the left and right  
390 dorsal caudate nodes are independently positively associated with network dynamic change;  
391 particularly related to enhancement of time spent in the DMN state. Translational research has  
392 established that the dopamine system and corticostriatal circuits, involving the dorsal caudate  
393 specifically, are implicated in addiction, ADHD, and the pharmacological action of MPH in the  
394 treatment of ADHD(48–51). More recent evidence has built on this historical understanding to  
395 illustrate that activity of neurocognitive networks, particularly DMN, is aberrant in these  
396 disorders(3,7,9,52,53). However, a gap remains in linking the often more pre-clinical body of

397 circuit-based evidence to large-scale brain network function. Our findings reveal a link between  
398 MPH-induced changes in functional corticostriatal circuitry and temporal dynamic function of  
399 the DMN. These results may suggest that dopaminergic agonism alters how cortical connections  
400 with the dorsal caudate are prioritized, leading to changes in temporal dynamic function of brain  
401 networks, particularly the DMN. If this is true, it would expand on theory that *static* DMN  
402 functional connectivity is modulated by D2/D3 receptors(3) and suggest a specific locus and  
403 mechanism of regulation at the dorsal caudate, a striatal region functionally defined by its role in  
404 cognitive control(28,54).

#### 405 Limitations

406 A limitation of this present work is that baseline dopaminergic function was not assessed  
407 using PET. This may be relevant as others have shown that individual variance in dopaminergic  
408 function may impact the action of MPH(55,56). However, the current participants were healthy  
409 with no clinical appearance of dopaminergic disruptions. We also used a within-subjects design,  
410 which reduces the impact of individual variance. While we defined a relationship between  
411 temporal dynamics and corticostriatal configuration, we relied on correlational analyses and are  
412 unable to determine a causal relationship between these changes. As articulated in the discussion,  
413 we speculated that changes in corticostriatal interactions may drive the influence of MPH on  
414 temporal dynamic function; this hypothesis needs to be confirmed in future work. However, even  
415 in the absence of a causal link, we provide comprehensive evidence of MPH's impact on  
416 temporal dynamics and related static resting state features that differ significantly from HAL.

#### 417 Conclusion

418           We find that pharmacological agents – MPH and HAL – have distinct impacts on  
419 network temporal dynamics and on corticostriatal configuration. Temporal dynamic findings  
420 suggest that MPH may prime the brain to engage in external or internal oriented attention,  
421 revealing a novel understanding of MPH action in alignment with the known impact of MPH on  
422 attention. Further, we show that while HAL does not alter corticostriatal configurations, MPH  
423 specifically alters ROR, acting to reshuffle the relative connectivity strength of multiple cortical  
424 regions with the striatum. The magnitude of this ‘reshuffling’, across the striatum and  
425 specifically at dorsal caudate is tied to MPH-induced change in brain network temporal  
426 dynamics, particularly the DMN. Thus, this work suggests that MPH-induced changes in dorsal  
427 caudate communication with the cortex may play a role in driving the time-varying engagement  
428 of the DMN and other large-scale brain networks, though future work is required to determine  
429 the causality of this association. Our findings ultimately uncover catecholamine-driven links  
430 between nuanced corticostriatal circuitry and large-scale brain network temporal dynamics,  
431 paving the way for a mechanistic understanding of the neurochemistry and neurocircuitry  
432 governing macro-scale brain network engagement.

433

434 **Acknowledgments**

435 This work was supported by the National Institute on Drug Abuse Intramural Research Program

436 We thank Dr. Blaise Frederick for his assistance in applying co-activation pattern analysis to this

437 data.

438 **Conflict of Interest**

439 The authors declare no conflict of interest.

440 **References**

- 441 1. Menon V, D'Esposito M. The role of PFC networks in cognitive control and executive  
442 function. *Neuropsychopharmacol.* 2022 Jan;47(1):90–103.
- 443 2. Menon V. Large-scale brain networks and psychopathology: a unifying triple network  
444 model. *Trends in Cognitive Sciences.* 2011 Oct 1;15(10):483–506.
- 445 3. Zhang R, Volkow ND. Brain default-mode network dysfunction in addiction. *NeuroImage.*  
446 2019 Oct 15;200:313–31.
- 447 4. Braun U, Harneit A, Pergola G, Menara T, Schäfer A, Betzel RF, et al. Brain network  
448 dynamics during working memory are modulated by dopamine and diminished in  
449 schizophrenia. *Nat Commun.* 2021 Jun 9;12(1):3478.
- 450 5. de la Cruz F, Wagner G, Schumann A, Suttkus S, Güllmar D, Reichenbach JR, et al.  
451 Interrelations between dopamine and serotonin producing sites and regions of the default  
452 mode network. *Hum Brain Mapp.* 2020 Oct 31;42(3):811–23.
- 453 6. Shafiei G, Zeighami Y, Clark CA, Coull JT, Nagano-Saito A, Leyton M, et al. Dopamine  
454 Signaling Modulates the Stability and Integration of Intrinsic Brain Networks. *Cerebral*  
455 *Cortex (New York, NY).* 2019 Jan;29(1):397.
- 456 7. Cai W, Chen T, Szegletes L, Supekar K, Menon V. Aberrant Time-Varying Cross-Network  
457 Interactions in Children With Attention-Deficit/Hyperactivity Disorder and the Relation to  
458 Attention Deficits. *Biological Psychiatry: Cognitive Neuroscience and Neuroimaging.* 2018  
459 Mar 1;3(3):263–73.
- 460 8. Mizuno Y, Cai W, Supekar K, Makita K, Takiguchi S, Tomoda A, et al. Methylphenidate  
461 remediates aberrant brain network dynamics in children with attention-deficit/hyperactivity  
462 disorder: A randomized controlled trial. *Neuroimage.* 2022 Aug 15;257:119332.
- 463 9. Quam A, Biernacki K, Ross TJ, Salmeron BJ, Janes AC. Childhood Trauma, Emotional  
464 Awareness, and Neural Correlates of Long-Term Nicotine Smoking. *JAMA Netw Open.*  
465 2024 Jan 11;7(1):e2351132.
- 466 10. Wang KS, Kaiser RH, Peechatka AL, Frederick BB, Janes AC. Temporal Dynamics of  
467 Large-Scale Networks Predict Neural Cue Reactivity and Cue-Induced Craving. *BPS: CNI.*  
468 2020 Nov 1;5(11):1011–8.
- 469 11. Wang KS, Brown K, Frederick BB, Moran LV, Olson D, Pizzagalli DA, et al. Nicotine  
470 acutely alters temporal properties of resting brain states. *Drug Alcohol Depend.* 2021 Sep  
471 1;226:108846.
- 472 12. Zhai T, Gu H, Salmeron BJ, Stein EA, Yang Y. Disrupted Dynamic Interactions Between  
473 Large-Scale Brain Networks in Cocaine Users Are Associated With Dependence Severity.  
474 *Biological Psychiatry: Cognitive Neuroscience and Neuroimaging.* 2023 Jun 1;8(6):672–9.

- 475 13. Kottaram A, Johnston L, Ganella E, Pantelis C, Kotagiri R, Zalesky A. Spatio-temporal  
476 dynamics of resting-state brain networks improve single-subject prediction of schizophrenia  
477 diagnosis. *Hum Brain Mapp.* 2018 Sep;39(9):3663–81.
- 478 14. Kottaram A, Johnston LA, Cocchi L, Ganella EP, Everall I, Pantelis C, et al. Brain network  
479 dynamics in schizophrenia: Reduced dynamism of the default mode network. *Hum Brain*  
480 *Mapp.* 2019 Jan 21;40(7):2212–28.
- 481 15. Janes AC, Peechatka AL, Frederick BB, Kaiser RH. Dynamic functioning of transient  
482 resting-state coactivation networks in the Human Connectome Project. *Human Brain*  
483 *Mapping.* 2020;41(2):373–87.
- 484 16. Kodama T, Kojima T, Honda Y, Hosokawa T, Tsutsui K ichiro, Watanabe M. Oral  
485 Administration of Methylphenidate (Ritalin) Affects Dopamine Release Differentially  
486 Between the Prefrontal Cortex and Striatum: A Microdialysis Study in the Monkey. *J*  
487 *Neurosci.* 2017 Mar 1;37(9):2387–94.
- 488 17. van den Bosch R, Lambregts B, Määttä J, Hofmans L, Papadopetraki D, Westbrook A, et al.  
489 Striatal dopamine dissociates methylphenidate effects on value-based versus surprise-based  
490 reversal learning. *Nat Commun.* 2022 Aug 24;13:4962.
- 491 18. Westbrook A, van den Bosch R, Määttä JI, Hofmans L, Papadopetraki D, Cools R, et al.  
492 Dopamine promotes cognitive effort by biasing the benefits versus costs of cognitive work.  
493 *Science.* 2020 Mar 20;367(6484):1362–6.
- 494 19. Wilens TE. Effects of Methylphenidate on the Catecholaminergic System in Attention-  
495 Deficit/Hyperactivity Disorder. *Journal of Clinical Psychopharmacology.* 2008  
496 Jun;28(3):S46.
- 497 20. Moyer JT, Wolf JA, Finkel LH. Effects of Dopaminergic Modulation on the Integrative  
498 Properties of the Ventral Striatal Medium Spiny Neuron. *Journal of Neurophysiology.* 2007  
499 Dec;98(6):3731–48.
- 500 21. Carter AG, Soler-Llavina GJ, Sabatini BL. Timing and location of synaptic inputs determine  
501 modes of subthreshold integration in striatal medium spiny neurons. *J Neurosci.* 2007 Aug  
502 15;27(33):8967–77.
- 503 22. Choi EY, Ding SL, Haber SN. Combinatorial Inputs to the Ventral Striatum from the  
504 Temporal Cortex, Frontal Cortex, and Amygdala: Implications for Segmenting the Striatum.  
505 *eNeuro.* 2017;4(6):ENEURO.0392-17.2017.
- 506 23. Korponay C, Choi EY, Haber SN. Corticostriatal Projections of Macaque Area 44. *Cereb*  
507 *Cortex Commun.* 2020 Nov 5;1(1):tgaa079.
- 508 24. Korponay C, Stein EA, Ross TJ. Misconfigured striatal connectivity profiles in smokers.  
509 *Neuropsychopharmacol.* 2022 Nov;47(12):2081–9.



- 510 25. Salimi-Khorshidi G, Douaud G, Beckmann CF, Glasser MF, Griffanti L, Smith SM.  
511 Automatic Denoising of Functional MRI Data: Combining Independent Component Analysis  
512 and Hierarchical Fusion of Classifiers. *NeuroImage*. 2014 Apr 4;90:449.
- 513 26. Griffanti L, Salimi-Khorshidi G, Beckmann CF, Auerbach EJ, Douaud G, Sexton CE, et al.  
514 ICA-based artefact and accelerated fMRI acquisition for improved Resting State Network  
515 imaging. *NeuroImage*. 2014 Jul 7;95:232.
- 516 27. Essen DCV, Smith SM, Barch DM, Behrens TEJ, Yacoub E, Ugurbil K, et al. The WU-Minn  
517 Human Connectome Project: An Overview. *NeuroImage*. 2013 Oct 10;80:62.
- 518 28. Choi EY, Yeo BTT, Buckner RL. The organization of the human striatum estimated by  
519 intrinsic functional connectivity. *J Neurophysiol*. 2012 Oct 15;108(8):2242–63.
- 520 29. Yeo BTT, Krienen FM, Sepulcre J, Sabuncu MR, Lashkari D, Hollinshead M, et al. The  
521 organization of the human cerebral cortex estimated by intrinsic functional connectivity.  
522 *Journal of Neurophysiology*. 2011 Sep;106(3):1125.
- 523 30. Tzourio-Mazoyer N, Landeau B, Papathanassiou D, Crivello F, Etard O, Delcroix N, et al.  
524 Automated Anatomical Labeling of Activations in SPM Using a Macroscopic Anatomical  
525 Parcellation of the MNI MRI Single-Subject Brain. *NeuroImage*. 2002 Jan;15(1):273–89.
- 526 31. Weber S, Aleman A, Hugdahl K. Involvement of the default mode network under varying  
527 levels of cognitive effort. *Sci Rep*. 2022 Apr 15;12(1):6303.
- 528 32. Hampson M, Driesen N, Roth JK, Gore JC, Constable RT. Functional connectivity between  
529 task-positive and task-negative brain areas and its relation to working memory performance.  
530 *Magnetic Resonance Imaging*. 2010 Oct 1;28(8):1051–7.
- 531 33. Sala-Llonch R, Peña-Gómez C, Arenaza-Urquijo EM, Vidal-Piñeiro D, Bargalló N, Junqué  
532 C, et al. Brain connectivity during resting state and subsequent working memory task  
533 predicts behavioural performance. *Cortex*. 2012 Oct 1;48(9):1187–96.
- 534 34. Sripada CS, Kessler D, Welsh R, Angstadt M, Liberzon I, Phan KL, et al. Distributed effects  
535 of methylphenidate on the network structure of the resting brain: A connectomic pattern  
536 classification analysis. *NeuroImage*. 2013 Nov 1;81:213–21.
- 537 35. Querne L, Fall S, Le Moing AG, Bourel-Ponchel E, Delignières A, Simonnot A, et al.  
538 Effects of Methylphenidate on Default-Mode Network/Task-Positive Network  
539 Synchronization in Children With ADHD. *J Atten Disord*. 2017 Dec 1;21(14):1208–20.
- 540 36. Diedenhofen B, Musch J. cocor: A Comprehensive Solution for the Statistical Comparison of  
541 Correlations. *PLOS ONE*. 2015 Apr 2;10(4):e0121945.
- 542 37. Spreng RN, Stevens WD, Chamberlain JP, Gilmore AW, Schacter DL. Default network  
543 activity, coupled with the frontoparietal control network, supports goal-directed cognition.  
544 *Neuroimage*. 2010 Oct 15;53(1):303–17.

- 545 38. Andrews-Hanna JR, Reidler JS, Sepulcre J, Poulin R, Buckner RL. Functional-Anatomic  
546 Fractionation of the Brain's Default Network. *Neuron*. 2010 Feb 25;65(4):550–62.
- 547 39. Buckner RL, Andrews-Hanna JR, Schacter DL. The Brain's Default Network. *Annals of the*  
548 *New York Academy of Sciences*. 2008;1124(1):1–38.
- 549 40. Turnbull A, Wang HT, Murphy C, Ho NSP, Wang X, Sormaz M, et al. Left dorsolateral  
550 prefrontal cortex supports context-dependent prioritisation of off-task thought. *Nat Commun*.  
551 2019 Aug 23;10:3816.
- 552 41. Newman SD, Carpenter PA, Varma S, Just MA. Frontal and parietal participation in problem  
553 solving in the Tower of London: fMRI and computational modeling of planning and high-  
554 level perception. *Neuropsychologia*. 2003 Jan 1;41(12):1668–82.
- 555 42. Goozee R, O'Daly O, Handley R, Reis Marques T, Taylor H, McQueen G, et al. Effects of  
556 aripiprazole and haloperidol on neural activation during a simple motor task in healthy  
557 individuals: A functional MRI study. *Hum Brain Mapp*. 2016 Dec 23;38(4):1833–45.
- 558 43. Volkow ND, Fowler JS, Wang GJ, Telang F, Logan J, Wong C, et al. Methylphenidate  
559 Decreased the Amount of Glucose Needed by the Brain to Perform a Cognitive Task. *PLoS*  
560 *One*. 2008 Apr 16;3(4):e2017.
- 561 44. Devaney KJ, Levin EJ, Tripathi V, Higgins JP, Lazar SW, Somers DC. Attention and  
562 Default Mode Network Assessments of Meditation Experience during Active Cognition and  
563 Rest. *Brain Sciences*. 2021 May;11(5):566.
- 564 45. Cattarinussi G, Di Giorgio A, Moretti F, Bondi E, Sambataro F. Dynamic functional  
565 connectivity in schizophrenia and bipolar disorder: A review of the evidence and  
566 associations with psychopathological features. *Progress in Neuro-Psychopharmacology and*  
567 *Biological Psychiatry*. 2023 Dec 20;127:110827.
- 568 46. Friston KJ. Functional and effective connectivity: a review. *Brain connectivity* [Internet].  
569 2011 [cited 2024 Jan 30];1(1). Available from: <https://pubmed.ncbi.nlm.nih.gov/22432952/>
- 570 47. Haber SN. The primate basal ganglia: parallel and integrative networks. *Journal of Chemical*  
571 *Neuroanatomy*. 2003 Dec 1;26(4):317–30.
- 572 48. King N, Floren S, Kharas N, Thomas M, Dafny N. Glutamatergic signaling in the caudate  
573 nucleus is required for behavioral sensitization to methylphenidate. *Pharmacol Biochem*  
574 *Behav*. 2019 Sep;184:172737.
- 575 49. Crawford CA, McDougall SA, Meier TL, Collins RL, Watson JB. Repeated methylphenidate  
576 treatment induces behavioral sensitization and decreases protein kinase A and dopamine-  
577 stimulated adenylyl cyclase activity in the dorsal striatum. *Psychopharmacology*. 1998 Feb  
578 1;136(1):34–43.
- 579 50. Volkow ND, Wang GJ, Newcorn J, Telang F, Solanto MV, Fowler JS, et al. Depressed  
580 Dopamine Activity in Caudate and Preliminary Evidence of Limbic Involvement in Adults

- 581 With Attention-Deficit/Hyperactivity Disorder. *Archives of General Psychiatry*. 2007 Aug  
582 1;64(8):932–40.
- 583 51. Schulz KP, Bédard ACV, Fan J, Hildebrandt TB, Stein MA, Ivanov I, et al. Striatal  
584 Activation Predicts Differential Therapeutic Responses to Methylphenidate and  
585 Atomoxetine. *Journal of the American Academy of Child & Adolescent Psychiatry*. 2017 Jul  
586 1;56(7):602-609.e2.
- 587 52. Broulidakis MJ, Golm D, Cortese S, Fairchild G, Sonuga-Barke E. Default mode network  
588 connectivity and attention-deficit/hyperactivity disorder in adolescence: Associations with  
589 delay aversion and temporal discounting, but not mind wandering. *International Journal of  
590 Psychophysiology*. 2022 Mar 1;173:38–44.
- 591 53. Picon FA, Sato JR, Anés M, Vedolin LM, Mazzola AA, Valentini BB, et al.  
592 Methylphenidate Alters Functional Connectivity of Default Mode Network in Drug-Naive  
593 Male Adults With ADHD. *J Atten Disord*. 2020 Feb;24(3):447–55.
- 594 54. Gordon EM, Laumann TO, Marek S, Newbold DJ, Hampton JM, Seider NA, et al.  
595 Individualized Functional Subnetworks Connect Human Striatum and Frontal Cortex. *Cereb  
596 Cortex*. 2021 Oct 28;32(13):2868–84.
- 597 55. Volkow ND, Wang GJ, Fowler JS, Logan J, Franceschi D, Maynard L, et al. Relationship  
598 between blockade of dopamine transporters by oral methylphenidate and the increases in  
599 extracellular dopamine: Therapeutic implications. *Synapse*. 2002;43(3):181–7.
- 600 56. Sayalı C, van den Bosch R, Määttä JI, Hofmans L, Papadopetraki D, Booij J, et al.  
601 Methylphenidate undermines or enhances divergent creativity depending on baseline  
602 dopamine synthesis capacity. *Neuropsychopharmacol*. 2023 Dec;48(13):1849–58.
- 603
- 604

605 Tables and Figures

606

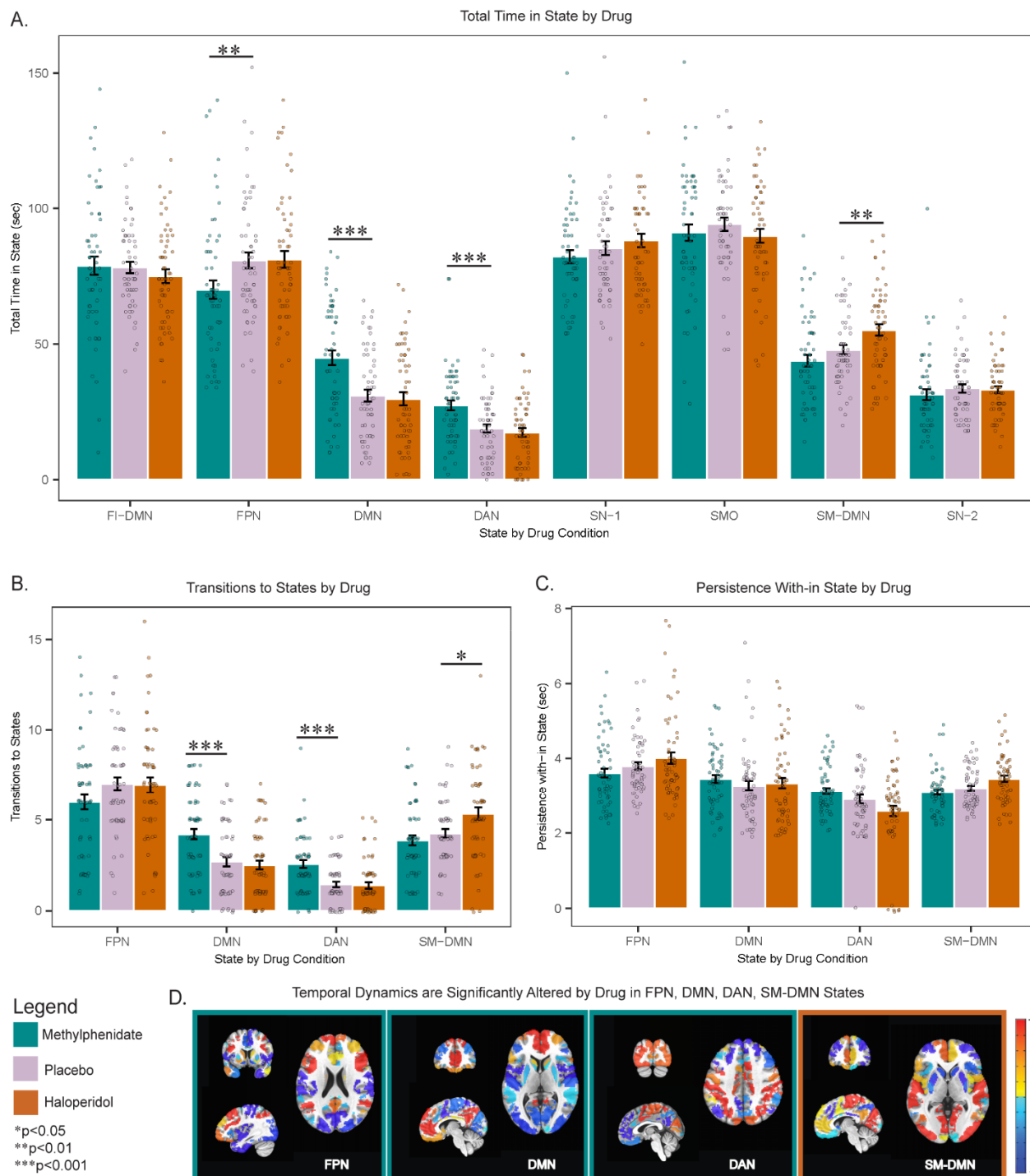
607 **Table 1.** Demographics of Sample

<b>Demographics</b>	
	<b>Healthy Controls (N = 59)</b>
Age (years)	39.32 ( <i>SD</i> = 11.25)
Sex (male/female)	17/42
Race ( <i>n</i> )	
Black/African American	11
White/Caucasian	37
Asian	5
More Than One Race	6
Ethnicity ( <i>n</i> )	
Hispanic	9
Non-Hispanic	49
Unknown or not reported	1
Education ( <i>n</i> )	
Less than High School	2
High School Complete/GED	8
Some / Partial Post-High School	22
College Graduate/Bachelor's Degree	18
Master's Degree	5
Professional Degree (MD, JD, Ph.D.)	4

608 Demographic characterization of sample.

609

610 Figure 1. Catecholaminergic Agents Significantly Alter Large-Scale Brain Network Temporal Dynamics

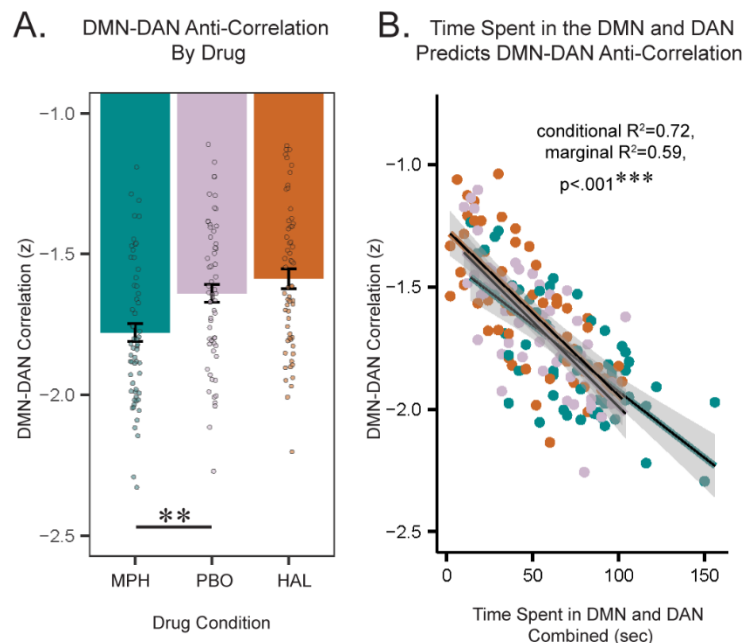


611 Figure 1. A. MPH increased time spent in DMN and DAN states and decreased time spent in FPN state.  
 612 HAL increased time spent in SM-DMN state. B. MPH increased transitions to DMN and DAN states while  
 614 HAL increased transitions to SM-DMN state. C. Neither MPH nor HAL altered time spent persisting within  
 615 DMN, DAN, FPN states or SM-DMN state. D. A visualization of FPN, DMN, DAN and SM-DMN states of  
 616 which dynamics are significantly altered by MPH (outlined in green) or HAL (outlined in orange). -1 is  
 617 most negative relative activation; +1 is most positive relative activation. MPH: methylphenidate; HAL:  
 618 haloperidol; FI-DMN: fronto-insular default mode network state; FPN: frontoparietal control network state;  
 619 DMN: default mode network state; DAN: dorsal attention network state; SN-1: salience network state 1;

620 SMO: sensory motor occipital state; SM-DMN: sensory motor default mode network state; SN-2 salience  
621 network state 2. \* $p_{\text{corr}} < 0.05$ , \*\* $p_{\text{corr}} < 0.01$ , \*\*\* $p_{\text{corr}} < 0.001$

622

623 Figure 2. DMN-DAN Static Anti-Correlation is Tied to DMN and DAN Temporal Function



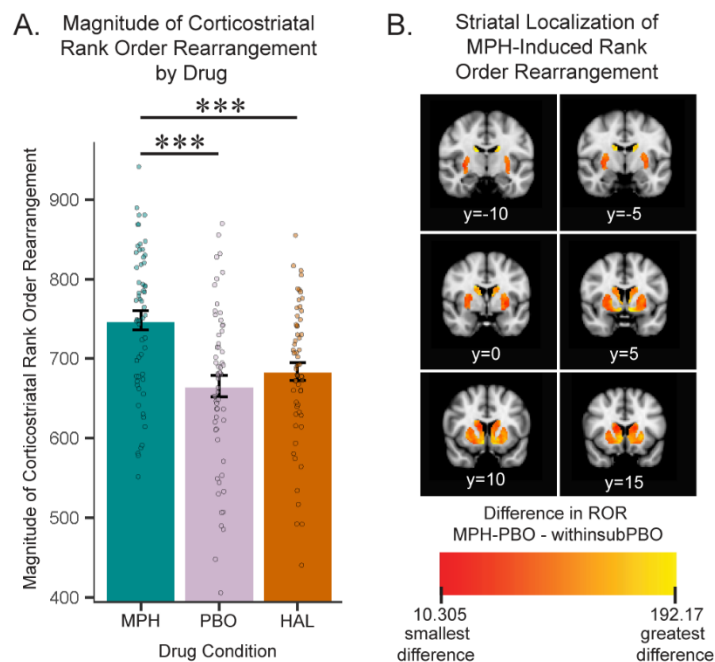
624

625 Figure 2. A. MPH significantly strengthens DMN-DAN anti-correlation. B. The combination of time spent in  
626 DMN and DAN negatively predicts DMN-DAN correlation values independently of drug. MPH:  
627 methylphenidate; HAL: haloperidol; DMN: default mode network; DAN: dorsal attention network.

628 \*\* $p_{\text{corr}} < 0.01$

629

630 Figure 3. Methylphenidate Significantly Heightens the Magnitude of Rank Order Rearrangement in  
631 Corticostriatal Connectivity Profile

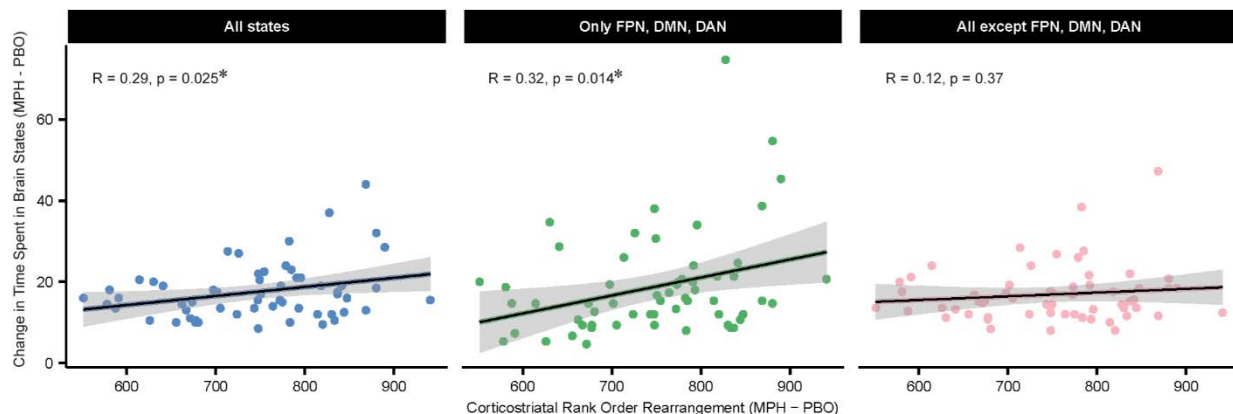


632  
633 Figure 3. A. Under MPH, there is significantly higher magnitude of ROR – measure of absolute change in  
634 relative corticostriatal connectivity - compared to placebo (within-session placebo rearrangement) and  
635 HAL (HAL-PBO rearrangement). B. Heatmap comparing magnitude of ROR at striatal voxels in MPH-  
636 PBO condition compared to within-session placebo condition. Across PBO and MPH conditions, relative  
637 connectivity strength between multiple cortical regions and the more red striatal voxels is more stable. In  
638 contrast, more yellow striatal voxels exhibit greater change in relative connectivity strength with cortical  
639 regions under MPH compared to PBO. ROR: rank order rearrangement; MPH: methylphenidate; HAL:  
640 haloperidol; PBO: placebo. \*\*\* $p_{\text{corr}} < 0.001$

641

642

643 Figure 4. Change in Network Temporal Dynamics is Related to Modulation of Functional Corticostriatal  
644 Circuitry under Methylphenidate



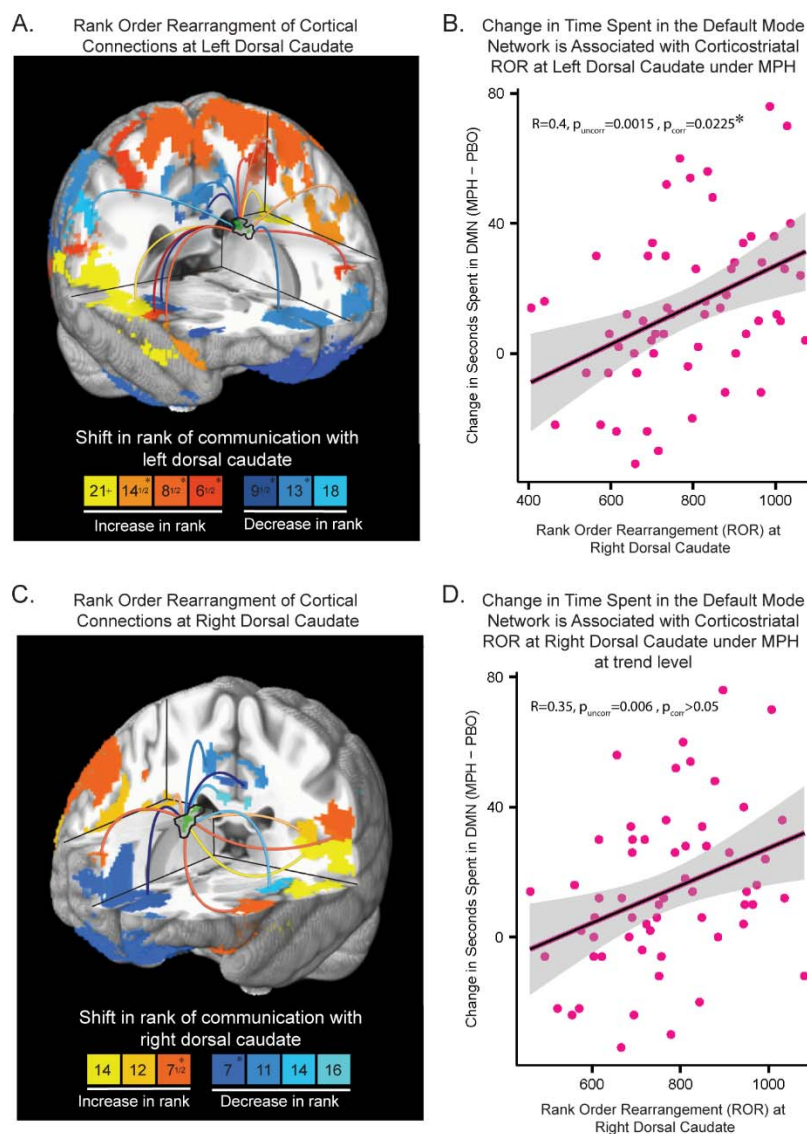
645  
646 Figure 4. Change in network temporal dynamics is associated with altered corticostriatal rank order  
647 rearrangement under MPH. Change in network temporal dynamics is operationalized as the sum, for  
648 each state tested, of the absolute value of the difference in total time spent in the state (MPH-PBO).  
649 Three panels vary by y-axis where left panel  $y =$  change in time spent in all states, middle panel  $y =$   
650 change in time spent in only FPN, DMN and DAN states, right panel  $y =$  change in time spent in all states  
651 except FPN, DMN, and DAN states. All Y-axis measures were divided by the number of states summed.  
652 MPH: methylphenidate, PBO: placebo; DMN: default mode network; DAN: dorsal attention network; FPN:  
653 frontoparietal network.

654

655



656 Figure 5. Methylphenidate-Induced Changes in the *Relative* Strength of Connectivity Between Cortical  
 657 Regions and the Dorsal Caudate is Associated with More Time Spent in the Default Mode Network under  
 658 Methylphenidate.



659

660 Figure 5. A and C. ROR at left dorsal caudate (A) and right dorsal caudate (C), depicting absolute change  
 661 in relative connectivity between multiple cortical regions and the dorsal caudate node under MPH  
 662 compared to PBO: Green regions are the data-driven striatal nodes of significant MPH-induced ROR  
 663 previously identified by a voxel-wise paired t-test. Cortical regions are color coded to depict how their  
 664 relative connectivity strength with the specified caudate node, or 'rank of communication', shifts under  
 665 MPH compared to under PBO. Regions shown shift at least 5 ranks. Color key at bottom indicates  
 666 magnitude of change in rank where \* indicates a mean magnitude of change for that color – this value  
 667 only varies by  $\pm 2$  values at maximum. Exact amount of change per significant cortical region is depicted in  
 668 supplementary material figure S3. B and D. Correlations between ROR at left dorsal caudate (B) and at  
 669 right dorsal caudate (D) and change in time spent (seconds) in the DMN under MPH compared to PBO.  
 670 MPH: methylphenidate; PBO: placebo; DMN: default mode network; \* $p_{\text{corr}} < 0.05$ .